arXiv:1404.2663v2 [hep-ph] 13 Jun 2014

Elliptic flow of thermal dileptons in event-by-event hydrodynamic simulation

Hao-jie Xu* and Qun Wang†
Department of Modern Physics, University of Science and Technology of China, Anhui 230026, People's Republic of China

Longgang Pang‡
Institute of Particle Physics and Key Laboratory of Quarks and Lepton Physics (MOE), Central China Normal University, Wuhan 430079, People's Republic of China

The elliptic flows of thermal di-electrons are investigated within a (2+1)-dimension event-by-event hydrodynamic model for Au+Au collisions at $\sqrt{s_{NN}} = 200$ GeV. The fluctuating initial conditions are given by the Monte Carlo Glauber model. We find in our event-by-event calculation rather weak correlation between the dilepton emission angles and the event plane angles of charged hadrons. We observe strong fluctuation effects in dilepton elliptic flows when using the event plane angles of dileptons at specific invariant mass M. The correlation between the dilepton event plane angle and charged hadron one becomes stronger with decreasing M. This provides a possible measure of the interplay between the effect of geometric deformation and that of fluctuating "hot spots" in relativistic heavy ion collisions.

I. INTRODUCTION

One of the most exciting phenomena found in high-energy heavy ion collisions (HIC) at Relativistic Heavy Ion Collider (RHIC) and the Large Hadron Collider (LHC) is the strong collective flow of final charged hadrons [1]. This is developed by fast expansion of Quark Gluon Plasma (QGP) and the Hadron Resonance Gas (HRG) in the early/later stage of the HIC. The collective flow not only contributes to the transverse momentum spectra of hadrons but also leads to the anisotropic distribution in the transverse plane. This anisotropy is the consequence of the pressure gradient in non-central collisions which drives the initial geometric asymmetry of the overlapping region of the colliding nuclei to the momentum anisotropy of final hadrons. The second Fourier coefficient of the azimuthal distribution is called the elliptic flow. The big elliptic flow measured at RHIC and LHC suggests fast local thermalization and the formation of strongly coupled QGP close to ideal fluid [2–4]. So the space-time evolution of the hot and dense matter can be described by hydrodynamic equations [5].

One critical input in hydrodynamic simulation is the initial condition. Recently many models such as Monte Carlo Glauber, Monte Carlo Color Glass Condensate, UrQMD, AMPT and EPOS are used to produce fluctuating initial conditions for event-by-event (EBE) hydrodynamic simulations [6–9]. These EBE calculations can explain odd harmonic flows like the triangle flow and the ridge structure in two-dimensional di-hadron correlation[10], they can also provide much better fit to the transverse momentum spectra and elliptic flows of charged hadrons at RHIC and LHC energy in both central and semi-central collisions [11–16] than smooth one-shot (SM) hydrodynamic simulation with smooth initial conditions.

Different from the strongly interacting hadrons which escape from the fireball only on the equal-temperature hypersurface at freeze-out, the electromagnetic probes like photons and dileptons, due to their instant emission once produced, are expected to provide undistorted information about the space-time information of the QGP and HRG matter [17–29]. The invariant mass spectra of dileptons are usually divided into the low, intermediate and high mass regions (LMR, IMR and HMR) based on the notion that each region is dominated by different sources of dileptons, thus provide a method to identify the different evolution stages of the expanding fireball.

The elliptic flows of dileptons have been studied in SM hydrodynamic simulations with smooth initial conditions[30–32]. However, the production rates of dileptons are sensitive to high temperature "hot spots" (fluctuations) in hot and dense medium. So the fluctuations are expected to play an important role in elliptic flows of dileptons in heavy ion collisions, which, to our knowledge, have never been investigated before. The aim of this paper is to calculate the elliptic flows of dileptons in an EBE hydrodynamic simulation with fluctuating initial conditions.

This paper is organized as follows. In Sec.II, we describe our EBE hydrodynamic model and use it to reproduce the transverse momentum spectra and elliptic flows of charged hadrons and compare to RHIC data. In Sec.III we calculate the invariant mass spectra and elliptic flows of dileptons from the EBE hydrodynamic simulation. We show the effect of fluctuations on dilepton elliptic flows with respect to the event plane defined by invariant mass dependent dilepton spectra and that defined by charged hadron spectra. We give a summary of our results in the final section.

II. EVENT-BY-EVENT HYDRODYNAMIC MODEL

We use a (2+1)-dimension ideal hydrodynamic model for the EBE simulation. Our model is similar to the AZHYDRO model [5, 9] which implements FCT-SHASTA algorithm[33, 34], but our codes are written in C++. The equation of state (EOS) with first order phase transition in the original AZHYDRO is replaced by Lattice QCD EOS which is pa-

*Electronic address: haojiexu@ustc.edu.cn
†Electronic address: qunwang@ustc.edu.cn
‡Electronic address: lgpang@iopp.ccnu.edu.cn

rameterized as S95P-PCE-v0 [35] with the chemical freeze-out temperature $T_{chem} = 165$ MeV. When the temperature of the medium is smaller than the kinetic freeze-out temperature T_f (which is set to 120 MeV in this study), the spectra of the directly produced hadrons are calculated by the Cooper-Frye formula [36] that mesons/baryons are emitted from the freeze-out hyper-surface defined by T_f following the Bose-Einstein/Fermi-Dirac distribution. We take more resonances [37] into account in our model than AZHYDRO. In order to calculate the dilepton spectra, we keep track of the local energy density and flow velocity profiles for the QGP and HRG matter during the evolution.

The Monte Carlo Glauber model [6] is employed to generate the profile of the fluctuating initial entropy density in Au+Au collisions at $\sqrt{s_{NN}} = 200$ GeV. In the Glauber model, the initial entropy density is assumed to be proportional to a linear combination of the number of participants $dN_{\rm part}/d^2\mathbf{x}_\perp$ and that of binary collisions $dN_{\rm coll}/d^2\mathbf{x}_\perp$[6],

$$\left.\frac{ds}{\tau_0 dx dy d\eta_s}\right|_{\eta_s=0} = \frac{C}{\tau_0}\left(\frac{1-\delta}{2}\frac{dN_{\rm part}}{d^2\mathbf{x}_\perp} + \delta\frac{dN_{\rm coll}}{d^2\mathbf{x}_\perp}\right), \quad (1)$$

where $C = 16$ and $\delta = 0.14$ are two constants, and the initial time is chosen to be τ_0 =0.4 fm/c. Since we use (2+1)-dimension hydrodynamic model with Bjorken boost-invariance [38] and focus on the central rapidity region, it is convenient to set the spatial rapidity η_s zero.

Normally the freeze-out hyper-surfaces are calculated in cuboidal way [5, 9, 39, 40] for each fluid cell. In the AZHYDRO model, in order to save the computing time, several fluid cells are used to generate a big piece of freeze-out hyper-surface. The flow velocity at the hyper-surface obtained in this way is an average of these cells. This will introduce numerical errors when the flow velocities are different for neighboring cells (especially with fluctuating initial conditions). In our model, we used a better treatment of the freeze-out hyper-surface. We first discretize the fluid velocity u^σ and then take the sum over the hyper-surface elements $\sum_{u_i^\sigma\in[u^\sigma,u^\sigma+du^\sigma]} d\Sigma_\mu^i$ for each fluid cell whose velocity is inside the bin $[u^\sigma, u^\sigma + du^\sigma]$ before carrying out the sum over different u^σ in the Cooper-Frye formula. This will substantially reduce the computing time while keeping the numerical accuracy with appropriately chosen bin size of the fluid velocity (the bin size is set to 0.02 in this paper). This method has been checked that it can reproduce the transverse momentum spectra and elliptic flows of hadrons.

The harmonic coefficients v_n which depend on transverse momenta are defined by

$$v_n(p_T) = \frac{\int_0^{2\pi} d\phi \frac{dN}{p_T dp_T d\phi dy}\cos[n(\phi-\Psi_n)]}{\int_0^{2\pi} d\phi \frac{dN}{p_T dp_T d\phi dy}}, \quad (2)$$

where Ψ_n are azimuthal angles of the event plane in momentum space

$$\Psi_n = \frac{1}{n}\arctan\frac{\langle p_T \sin(n\phi)\rangle}{\langle p_T\cos(n\phi)\rangle}. \quad (3)$$

Table I: Centralities and numbers of participants for Au+Au@$\sqrt{s}$ = 200 GeV calculated in one million events. The centrality bins are determined by number of participants $N_{\rm part}$. Here $N_{\rm part}^{\rm min}$ corresponds to the upper bound of the centrality bin.

Cnt	0-10%	10-20%	20-30%	30-40%	40-50%	50-60%
$N_{\rm part}^{\rm min}$	277	199	140	95	61	37

Here the average is taken over final charged hadrons in one event. The second and third harmonic coefficient are often called elliptic and triangle flow.

In Fig. 1 we show the p_T spectra and elliptic flow of charged hadrons for both EBE (400 events for each centrality bins) and SM hydrodynamic simulation in a variety of centralities. The centrality bins are determined by the number of participants $N_{\rm part}$ in Tab.I. The results are compared to the PHENIX data [41, 42]. In the SM case, the event-averaged initial entropy density distributions are used in the hydrodynamic calculation. We use the reaction plane as reference to take event average in the SM simulation. Another method is to use the participant plane. The two methods are different in elliptic flow for most central collisions [9, 14, 16].

We see in Fig. 1(a) that the p_T spectra of charged hadrons in the EBE simulation is harder than the SM simulation in each centrality bin. The better agreement of the EBE result with data is due to the bigger pressure gradient produced from the "hot spots" which drives bigger collective flows in the early stage of hydrodynamic evolution [9, 14]. Charged hadron spectra are only sensitive to those "hot spots" which are close to the freeze-out hyper-surface, while thermal photon and dilepton spectra are influenced by all "hot spots" in whole space-time volume.

In Fig. 1(b), we see that the elliptic flows in the EBE case are lower than the SM results in semi-central and peripheral collisions, while they are higher than the SM results in central collisions. This clearly shows the fluctuation effect on the elliptic flow. We know that the elliptic flow is the result of geometric eccentricity and initial fluctuation. The geometric eccentricity gives a non-zero elliptic flow, while hot spot fluctuation gives almost an isotopic flow. In semi-central and peripheral collisions, the geometric eccentricity in the SM case is slightly smaller than that in the EBE case. The fluctuation effect greatly reduces the elliptic flow in the EBE case. In central collisions, the deviation of the participant plane from the reaction plane is larger for central collisions than peripheral collisions, so the eccentricity in the SM case is much smaller than that in the EBE case [16], which gives much smaller elliptic flow in the SM case even with the reduction effect from fluctuation in the EBE calculation.

To identify whether the harmonic flow is generated by geometric eccentricity or fluctuating "hot spots", it is worth to study the azimuthal angle distribution of the event plane. In our hydrodynamic simulation, the reaction plane's azimuthal angle is set to 0. In Fig. 2, we show the distribution associated with the second and third harmonic flows at centrality $20-30\%$ by using 1000 hydrodynamic events with fluctuating initial energy density distributions. We see that Ψ_3

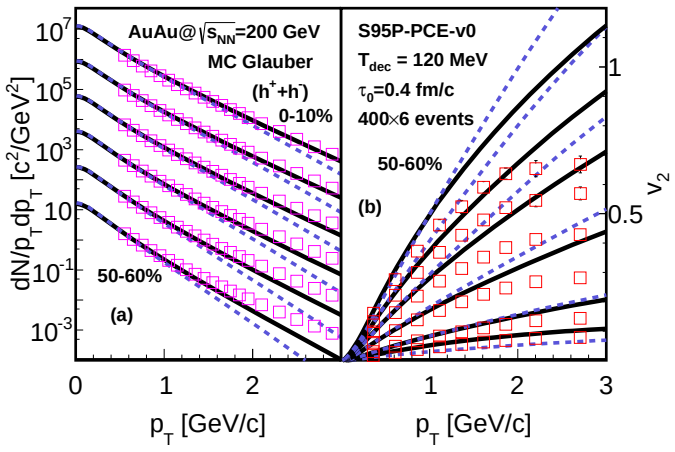

Figure 1: (Color online) (a) Transverse momentum spectra and (b) elliptic flows v_2 for charged hadrons as functions of p_T in different centrality bins for Au+Au collisions at $\sqrt{s_{NN}} = 200$ GeV. The hydrodynamic simulations are done with fluctuating (black-solid lines) and smooth(blue-dash lines) initial conditions. In the top-down order, the curves correspond to centrality bins (a) $(0-10\%)\times 10^4$, $(10-20\%)\times 10^3$, $(20-30\%)\times 10^2$, $(30-40\%)\times 10$, $(40-50\%)$, $(50-60\%)\times 0.1$ and (b) $(50-60\%)\times 3$, $(40-50\%)\times 2.5$, $(30-40\%)\times 2$, $(20-30\%)\times 1.5$, $(10-20\%)$, $(0-10\%)$, where the number outside the parenthesis denotes the normalization factor of each curve. The data (symbols) are taken from the PHENIX collaboration[41, 42].

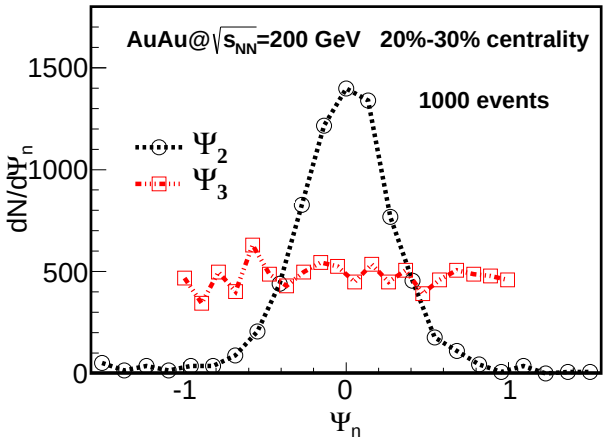

Figure 2: (Color online) The 2nd and 3rd event plane azimuthal angle distribution from EBE hydrodynamic simulation with 1000 fluctuating events.

are completely uncorrelated with the reaction plane. The decorrelation indicates that the triangle flows are mostly generated by fluctuating "hot spots". However Ψ_2 are strongly correlated with the reaction plane as expected since v_2 is actually a collective flow response to the geometric deformation [14] in semi-central and peripheral collisions.

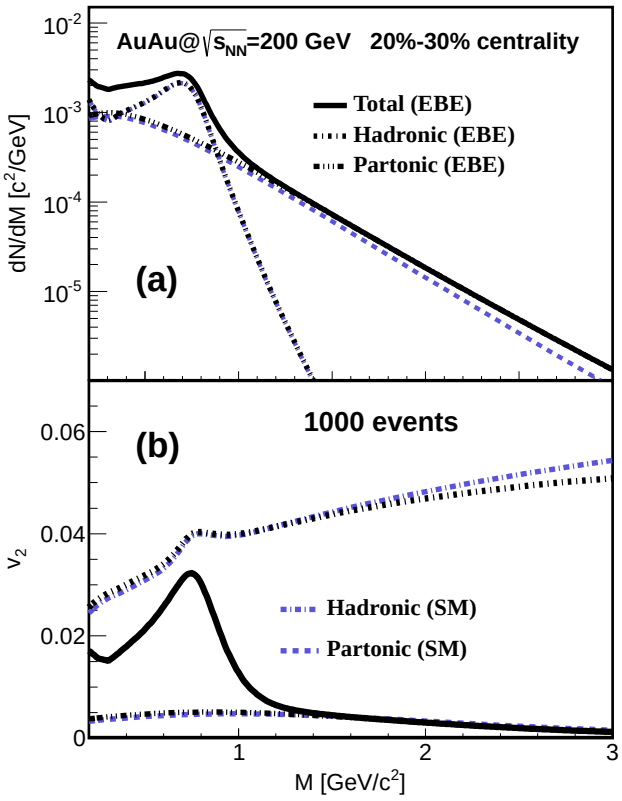

Figure 3: (Color online) (a) Invariant mass spectra and (b) elliptic flows of di-electrons in semi-central Au+Au collisions at $\sqrt{s_{NN}}$ =200 GeV.

III. ELLIPTIC FLOW OF THERMAL DILEPTONS

The differential production rate of dileptons per unit volume can be written in the following form (see, e.g. [21, 25]),

$$\frac{dN}{d^4x d^4p} = -\frac{\alpha}{4\pi^2}\frac{1}{M^2} n_B(p\cdot u)\left(1+\frac{2m_l^2}{M^2}\right) \times\sqrt{1-\frac{4m_l^2}{M^2}}\,\mathrm{Im}\Pi^R(p,T). \quad (4)$$

Here m_l is the lepton mass, α is fine structure constant, p is the dilepton's four momentum and $M\equiv\sqrt{p^2}$ is the dilepton invariant mass, $n_B(p\cdot u)\equiv 1/(\exp(p\cdot u/T)-1)$ (T and u are the local temperature and fluid velocity, respectively) is the Bose-Einstein distribution function, and Π^R is the retarded polarization tensor from the quark loop in the QGP phase or the hadronic loop in the HRG phase. In the HRG phase, the thermal dilepton production rate is dominated by in-medium ρ meson decays. The details of the calculation of dilepton invariant mass spectra in Au+Au collisions at the RHIC energy are given in Ref. [24, 31] by some of us. To simplify our calculation, we will focus on $20-30\%$ centrality bin and neglect the contribution from in-medium ω and ϕ meson decays.

In Fig. 3(a) we show the invariant mass spectra of di-electrons in semi-central ($20-30\%$ centrality bin) Au+Au

collisions at the RHIC energy. The LMR thermal dilepton production rate is dominated by in-medium ρ decays. The broadened dilepton invariant mass spectra around the mass of the free ρ indicate a strong medium modification by scatterings between ρ and other mesons and baryons in thermal medium. This modification is described by using hadronic many body theory[43] and empirical scattering amplitude method [44]. In the IMR the dileptons from QGP are dominant, and more dileptons are produced in the QGP phase in the EBE calculation (dash-dot-dot-dotted line, overlapping with the solid line) than the SM calculation (dashed). Such an enhancement is due to the "hot spots" in fluctuating initial conditions where larger-than-average temperature give a large contribution to the HMR dieltpon. Similar results were found in the EBE calculation for thermal photons [17]. The fluctuation effect on the invariant mass spectra in the HRG phase is negligible, since most of hadronic dileptons are produced later than the partonic ones [31] and the HRG phase only appears below the transition temperature.

The differential elliptic flow coefficient $v_2(M)$ as a function of the invariant mass is given by

$$v_2(M) = \frac{\int d\phi (dN/dMd\phi dy)\cos(2(\phi - \Psi_2))}{\int d\phi (dN/dMd\phi dy)}, \qquad (5)$$

where Ψ_n with $n = 2$ is the azimuthal angle of the event plane for final state charged hadrons in momentum space as defined in Eq. (3). The $v_2(M)$ results are shown in Fig. 3(b). We see in the figure that the elliptic flows of dileptons in the HRG phase in the EBE and SM case increase with M. The small peak in the hadronic component around the ρ mass is due to the temperature-dependent in-medium ρ meson spectral functions. The elliptic flow in the QGP phase is much smaller than that in the HRG phase, since the QGP phase is in the early stage of the fireball evolution before the transverse flow is fully developed. The sharp decrease of the elliptic flow from the HGR dominated region to the QGP dominated region can be a possible signal for QGP formation in heavy ion collisions [31].

As shown in Fig. 3(b), the elliptic flow with the fluctuating initial condition in the LMR/HMR is slightly larger/smaller than that without fluctuation. Such a small fluctuation effect is beyond our expectation since most IMR and HMR dileptons are produced at early time of the fireball expansion and their harmonic flow should be sensitive to the initial fluctuating "hot-spots". The reason is that the dilepton elliptic flow is calculated with respect to the event plane azimuthal angle Ψ_2 for final charged hadrons according to Eq. (5), however Ψ_2 is strongly correlated to the initial geometric deformation but not to dilepton azimuthal angles with the fluctuating initial condition.

To support the above reasoning, we introduce the following event plane azimuthal angle $\varphi_n(M)$ for dileptons,

$$\varphi_n(M) = \frac{1}{n}\arctan\frac{\langle p_T \sin(n\phi)\rangle}{\langle p_T \cos(n\phi)\rangle}. \qquad (6)$$

Here the average is taken over thermal dileptons at specific mass in one event. In Fig. (4) we show the distribution

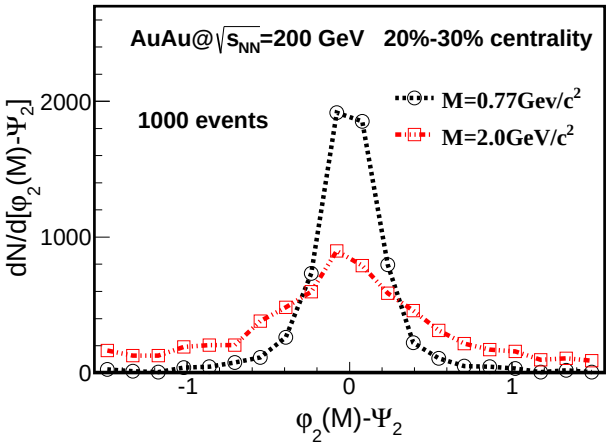

Figure 4: (Color online) The distribution of $\varphi_2 - \Psi_2$ at dilepton invariant mass $M = 0.77$ GeV/c^2 and $M = 2$ GeV/c^2 in EBE hydrodynamic simulation with the same 1000 events as in Fig. (2). φ_2/Ψ_2 is the event plane azimuthal angle defined by dileptons/hadrons.

of $\varphi_2(M) - \Psi_2$ for thermal dileptons at $M = 0.77$ GeV/c^2 (hadronic dominated region) and $M = 2.0$ GeV/c^2 (partonic dominated region) with the same events as in Fig. (2). It is obvious that the correlation of $\varphi_2(M)$ and Ψ_2 is much stronger in the HRG phase than that in the QGP phase. In this case, when we choose the event plane angle Ψ_2 of charged hadrons to calculate the dilepton elliptic flow at $M = 2.0$ GeV/c^2, the fluctuation effect is washed out by the weak correlation of $\varphi_2(M)$ and Ψ_2. The de-correlation of $\varphi_2(M)$ and Ψ_2 is due to the interplay of the geometric deformation and fluctuating initial "hot spots". In the early stage, the elliptic flow is small and the de-correlation effect is large, while in the later hadronic stage, the elliptic flow is driven by the geometric deformation and the de-correlation effect becomes weaker. The correlation between $\varphi_2(M)$ and Ψ_2 becomes stronger from higher mass to lower mass. This provides us with a measure of the interplay between the effect of geometric deformation and that of fluctuating "hot spots" in relativistic heavy ion collisions.

To look at the effect of replacing Ψ_2 with $\varphi_2(M)$, we can define the dilepton elliptic flow as

$$v_2(M) = \frac{\int d\phi (dN/dMd\phi dy)\cos(2(\phi - \varphi_2(M))}{\int d\phi (dN/dMd\phi dy)}. \qquad (7)$$

Fig. (5) shows the big difference between the $v_2(M)$ results with $\varphi_2(M)$ and that with Ψ_2 in the EBE hydrodynamic simulation. This difference is due to the strong de-correlation between Ψ_2 and $\varphi_2(M)$. Notice that the contribution from hadronic phase to Eq. (7) is below that to Eq. (5) at $M > 1.2$ GeV/c^2. This is because the dilepton production rate at high mass region is dominated by the partonic contribution, the dilepton event plane defined by Eq. (6) in that mass region is almost that of dileptons from partonic phase instead of hadronic phase. Therefore when looking at v_2 of dileptons from hadronic phase in high mass region, it is more correlated to the orientation of charged hadrons than to that of dilep-

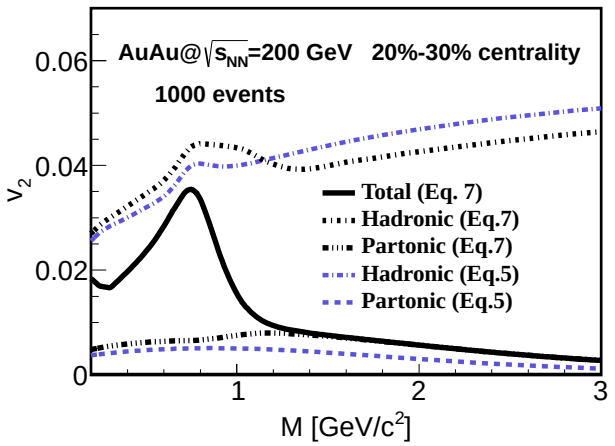

Figure 5: (Color online) The elliptic flows of di-electrons in semi-central Au+Au collisions at $\sqrt{s_{NN}}$ =200 GeV with the event plane azimuthal angles defined by dileptons at specific M.

tons mainly from partonic phase. Mathematically the mean value of $|\varphi_h(M) - \varphi_2(M)|$ in Eq. (7) is bigger than that of $|\varphi_h(M) - \Psi_2|$ in Eq. (5) at high mass region which will bring a smaller v_2, where $\varphi_h(M)$ is the azimuthal angle of dilepton from hadronic phase at specific mass. The de-correlation suggests that the importance of the choices of event planes in maximizing the dilepton elliptic flows. In experiments, however, it is difficult to identify the dilepton event planes because of very low production rates dileptons.

The de-correlation effects are also present for final charged hadrons. In a recent work on two-particle correlation [45], it was pointed out that the flow angle Ψ_n may depend on the transverse momentum p_T and the pseudo-rapidity η. The p_T-dependent event plane angle for charged hadrons have also been studied in Ref. [46]. Similar de-correlation effect was found in thermal photon elliptic flows with viscous hydrodynamic simulation [23], where the event angle Ψ_n from pions de-correlate from $\Psi_n^{\gamma}(p_T)$ defined by thermal photons at specific p_T. While in our work, we realize the evolution of de-correlation effect in relativistic heavy ion collisions.

IV. SUMMARY AND CONCLUSION

We investigated the elliptic flows of di-electrons in Au+Au collisions at $\sqrt{s_{NN}} = 200$ GeV by using a (2+1)-dimension event-by-event hydrodynamic model. The fluctuating initial entropy density profile is generated by the Monte Carlo Glauber model. The event-by-event hydrodynamic simulation gives a better description of transverse momentum spectra and elliptic flows of final charged hadrons in central and semi-central collisions. The event plane angle distribution indicates that the elliptic flow is largely generated by the initial geometric deformation while the triangle flow is largely generated by initial fluctuating "hot spots".

The dilepton invariant mass spectra are harder in the HMR from event-by-event hydrodynamic simulation than the one-shot results, which is due to larger-than-average temperatures of fluctuating "hot spots". The fluctuation effects are small when we use the event plane angle from final charged hadrons in calculating dilepton elliptic flows.

We observed bigger fluctuation effects when we used event plane angles defined by dileptons at specific M. The correlation between the event plane angle of dileptons at specific M and that of charged hadrons becomes stronger with decreasing M. This provides us with a possible measure of the interplay between the effect of geometric deformation and that of fluctuating "hot spots" in relativistic heavy ion collisions.

Acknowledgments

This work is supported partially by the National Natural Science Foundation of China projects (No. 11125524) and the Major State Basic Research Development Program in China (No. 2014CB845402)

[1] J.-Y. Ollitrault, Phys.Rev. **D46**, 229 (1992).
[2] K. Ackermann et al. (STAR Collaboration), Phys.Rev.Lett. **86**, 402 (2001).
[3] K. Adcox et al. (PHENIX Collaboration), Phys.Rev.Lett. **89**, 212301 (2002).
[4] K. Aamodt et al. (ALICE Collaboration), Phys.Rev.Lett. **105**, 252302 (2010).
[5] P. F. Kolb, J. Sollfrank, and U. W. Heinz, Phys.Rev. **C62**, 054909 (2000).
[6] T. Hirano and Y. Nara, Phys.Rev. **C79**, 064904 (2009).
[7] J. Steinheimer, V. Dexheimer, H. Petersen, M. Bleicher, S. Schramm, et al., Phys.Rev. **C81**, 044913 (2010).
[8] K. Werner, I. Karpenko, T. Pierog, M. Bleicher, and K. Mikhailov, Phys.Rev. **C82**, 044904 (2010).
[9] L. Pang, Q. Wang, and X.-N. Wang, Phys.Rev. **C86**, 024911 (2012).
[10] L. Pang, Q. Wang, and X.-N. Wang (2013), 1309.6735.
[11] B. Alver, B. Back, M. Baker, M. Ballintijn, D. Barton, et al., Phys.Rev. **C77**, 014906 (2008).
[12] H. Holopainen, H. Niemi, and K. J. Eskola, Phys.Rev. **C83**, 034901 (2011).
[13] J. Jia (ATLAS Collaboration), Nuclear Physics A **910-911**, 276 (2013).
[14] Z. Qiu and U. W. Heinz, Phys.Rev. **C84**, 024911 (2011).
[15] Z. Qiu and U. Heinz, Phys.Lett. **B717**, 261 (2012).
[16] B. Schenke, S. Jeon, and C. Gale, Phys.Rev.Lett. **106**, 042301 (2011).
[17] R. Chatterjee, H. Holopainen, T. Renk, and K. J. Eskola, Phys.Rev. **C83**, 054908 (2011).
[18] R. Chatterjee, H. Holopainen, I. Helenius, T. Renk, and K. J. Eskola, Phys.Rev. **C88**, 034901 (2013).
[19] K. Kajantie, J. I. Kapusta, L. D. McLerran, and A. Mekjian,

Phys.Rev. **D34**, 2746 (1986).
[20] O. Linnyk, W. Cassing, J. Manninen, E. Bratkovskaya, and C. Ko, Phys.Rev. **C85**, 024910 (2012).
[21] L. D. McLerran and T. Toimela, Phys.Rev. **D31**, 545 (1985).
[22] J. Ruppert, C. Gale, T. Renk, P. Lichard, and J. I. Kapusta, Phys.Rev.Lett. **100**, 162301 (2008).
[23] C. Shen, U. W. Heinz, J.-F. Paquet, I. Kozlov, and C. Gale (2013), 1308.2111.
[24] H.-j. Xu, H.-f. Chen, X. Dong, Q. Wang, and Y.-f. Zhang, Phys.Rev. **C85**, 024906 (2012).
[25] H. van Hees and R. Rapp, Nucl.Phys. **A806**, 339 (2008).
[26] H. van Hees and R. Rapp, Phys.Rev.Lett. **97**, 102301 (2006).
[27] G. Vujanovic, C. Young, B. Schenke, R. Rapp, S. Jeon, et al., Phys.Rev. **C89**, 034904 (2014).
[28] H.-j. Xu, X. Dong, L.-j. Ruan, Q. Wang, Z.-b. Xu, et al., Phys.Rev. **C89**, 024905 (2014).
[29] L. Adamczyk et al. (STAR Collaboration) (2014), 1402.1791.
[30] P. Mohanty, V. Roy, S. Ghosh, S. K. Das, B. Mohanty, et al., Phys.Rev. **C85**, 031903 (2012).
[31] J. Deng, Q. Wang, N. Xu, and P. Zhuang, Phys.Lett. **B701**, 581 (2011).
[32] R. Chatterjee, D. K. Srivastava, U. W. Heinz, and C. Gale, Phys.Rev. **C75**, 054909 (2007).
[33] J. P. Boris and D. L. Book, Journal of computational physics **11**, 38 (1973).
[34] S. T. Zalesak, Journal of computational physics **31**, 335 (1979).
[35] P. Huovinen and P. Petreczky, Nucl.Phys. **A837**, 26 (2010).
[36] F. Cooper and G. Frye, Phys.Rev. **D10**, 186 (1974).
[37] S. Eidelman et al. (Particle Data Group), Phys.Lett. **B592**, 1 (2004).
[38] J. Bjorken, Phys.Rev. **D27**, 140 (1983).
[39] T. Hirano, Phys.Rev. **C65**, 011901 (2001).
[40] B. Schenke, S. Jeon, and C. Gale, Phys.Rev. **C82**, 014903 (2010).
[41] S. Adler et al. (PHENIX Collaboration), Phys.Rev. **C69**, 034910 (2004).
[42] A. Adare et al. (PHENIX Collaboration), Phys.Rev.Lett. **107**, 252301 (2011).
[43] R. Rapp, Phys.Rev. **C63**, 054907 (2001).
[44] V. Eletsky, M. Belkacem, P. Ellis, and J. I. Kapusta, Phys.Rev. **C64**, 035202 (2001).
[45] F. G. Gardim, F. Grassi, M. Luzum, and J.-Y. Ollitrault, Phys.Rev. **C87**, 031901 (2013).
[46] U. Heinz, Z. Qiu, and C. Shen, Phys.Rev. **C87**, 034913 (2013).